INTEGRATED SOLAR COLLECTOR STORAGE SYSTEM BASED ON A SALT-HYDRATE PHASE-CHANGE MATERIAL

Y. RABIN,*† I. BAR-NIV,* E. KORIN*‡ and B. MIKIC**
*Department of Chemical Engineering, Ben-Gurion University of the Negev, P.O. Box 653, Beer-Sheva
84105, Israel and **Department of Mechanical Engineering, Massachusetts Institute of Technology,
Cambridge, MA 02139, U.S.A.

Abstract—A new integrated collector storage (ICS) concept for low-temperature solar heating of water is described. The solar energy is stored in a salt-hydrate phase-change material (PCM) held in the collector and is discharged to cold water flowing through a surface heat exchanger located in a layer of stationary heat transfer liquid (SHTL), floating over an immiscible layer of PCM. A theoretical model for the charging process of the proposed integrated collector is presented. The model assumes one-dimensional transient heat conduction in the PCM and SHTL layers and neglects the effect of convection heat transfer in these regions. The model was solved numerically by an enthalpy-based finite differences method and validated against experimental data. The results of parametric studies on the effect of the transition temperature and of the thickness layer of the salt-hydrate PCM on the thermal performance of the charging process are also presented.

1. INTRODUCTION

The integrated collector storage (ICS) concept is considered to be a promising direction for increasing the economic feasibility of low-temperature solar systems for heating water for domestic, agricultural and industrial applications. A system of this type combines collection and storage of thermal energy in a single unit. Compared with the conventional domestic water heating system, the integrated collector has the advantage of simplicity, both in erection and in operation. However, it has a relatively low efficiency (Bar-Cohen, 1978; Shmidt *et al.*, 1988). Boy *et al.* (1987) proposed an ICS system based on a salt-hydrate phase-change material (PCM) as an appliance for providing hot water instantaneously. They demonstrated that the thermal efficiency of such system could be improved significantly by incorporating an appropriate PCM device. However, in their system the salt-hydrate PCM was encapsulated in a special corrugated-fin heat exchanger, which increased the cost of the system.

In the present work we propose a new type of integrated collector module that does not require a water/PCM surface heat exchanger but uses a water/organic liquid (oil) heat exchanger instead. A schematic representation

of the proposed apparatus—the ICS-PCM module—is given in Fig. 1. The system consists of a thermally insulated plastic container, containing a layer of stationary heat transfer liquid (SHTL), floating over a layer of an immiscible salt-hydrate PCM (the density of the SHTL is obviously lower than that of the liquid salt hydrate). A finned heat exchanger located in the SHTL is used to heat cold water during the discharging process. The SHTL is covered with a metal plate coated with a selective absorbing film and with a transparent insulating lid. As the PCM melts, its density decreases and its volume thus increases. The SHTL displaced as a consequence of this expansion is stored in a
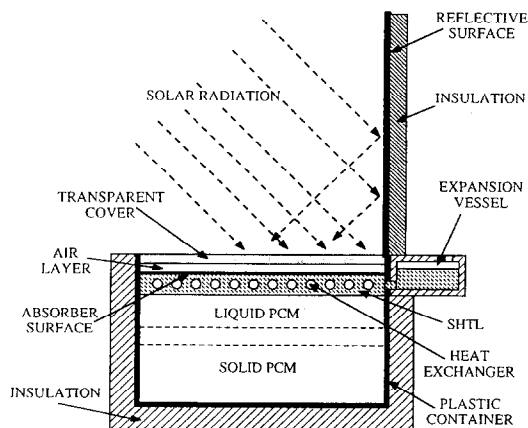

Fig. 1. Schematic presentation of the integrated solar collector storage system based on a phase-change material (ICS-PCM).

---

†Present address: Department of Mechanical Engineering, Carnegie-Mellon University, Pittsburgh, PA 15213, U.S.A.
‡ISES member to whom correspondence should be addressed.

small interconnecting chamber, designated the expansion vessel. A removable cover made of a material with a low thermal conductivity and coated on one side with a reflective material may be used as an optional extra to increase solar energy absorption during the day, as shown in Fig. 1. It may also be used as additional cover to reduce heat loss during the night.

The charging process taking place during the day is based on the absorption of the solar radiation by the selective surface and heat transfer to the PCM through the SHTL layer, mainly by conduction. This process causes the PCM to melt. The discharging process, which is based on the falling crystal method (FCM) (Greene, 1978; MacCraken, 1981; Korin and Mikic, 1989) takes place as follows. As the temperature at the SHTL/PCM interface drops below the solidification temperature, solid species are formed in the PCM. Under appropriate design and operation conditions, the solid crystal seperate from the SHTL/PCM interface and sink to the bottom of the container under the influence of gravity. "Fresh" liquid species thus come into contact at the interface, and the cycle is repeated. The direct contact between the SHTL and liquid salt hydrate facilitates good thermal contact. Heat released in this way is transferred to the cold water flowing through a finned-coil heat exchanger located in the SHTL layer.

The main advantages of the proposed ICS-PCM method are: (a) the system does not require an expensive phase-change surface heat exchanger; (b) the water/oil heat exchanger does not come into contact with the salt-hydrate and therefore corrosion problems are prevented; (c) in cold areas anti-freeze protection is not required; and (d) the system is simple, and there are no special requirements for maintenance and operation. The main disadvantages of the system are: (a) application of this method is limited to those salt hydrate PCMs that have large differences between their solid and liquid densities; and (b) the discharge process depends on the kinetics of crystallization of the chosen salt hydrate PCM. [Relevant mass transfer problems with their possible solutions related to the discharging process are given in Korin and Mikic (1989).] These drawbacks limit the possible applications of this method to special cases.

We thus intend to develop the system for solar heating of water to relatively low temperatures for applications such as space and root

zone heating in protected cultivation. For example in a closed greenhouse located in an arid region (such as in the area of Beer-Sheva, Israel), the air temperature inside the building may rise to >35°C on a typical clear winter's day and drop during the night to values close to the ambient minimum night temperature, which is usually in the range of 4–5°C (Korin et al., 1987). On a clear cold night, due to intensive radiation to the sky, the minimum night temperature may even fall below 0°C. To obtain the desirable indoor temperature, which is specific to each type of crop, (e.g. melons 12–35°C, tomatoes 10–30°C, roses 16–28°C) the greenhouse has to be equipped with cooling and heating systems. In many cases, a low-temperature energy source (18–25°C) would be sufficient for keeping the night temperature above the required minimum. For example, to maintain the air temperature above 12°C when the outside temperature is 0–5°C, a heat source of 20°C would be sufficient. The ICS-PCM system could be used to supply warm water at a relatively low temperature for keeping the night temperature in the greenhouse above the minimum required. The system could also be used in combination with an other solar system, such as passive solar plastic water sleeves (Zabeltitz, 1989), or a selective radiation filter solution in forced circulation (Kopel et al., 1991).

This paper focuses mainly on the study of solar charging process in the ICS-PCM system, and includes the following aspects: (1) a theoretical model for thermal analysis of the charging process in the ICS-PCM; (2) validation testing of the theoretical model versus data obtained from an experimental module; and (3) theoretical parametric studies related to the phase-change transition temperature and the thickness of the PCM layer.

2. THEORETICAL MODEL FOR THE CHARGING PROCESS

A schematic description of the ICS-PCM during the energy charging period is presented in Fig. 2. The model relates to a multilayer system consisting of the following elements: a transparent cover, an air layer, a selective absorber plate, a SHTL, a PCM salt-hydrate layer, and a thermal insulation layer. The model assumes temperature-dependent thermophysical properties and time-dependent meteorological parameters, i.e. solar intensity, ambient temperature, and wind velocity.
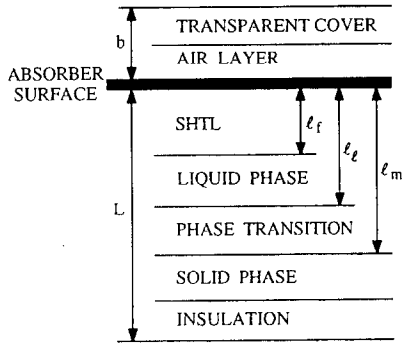
Fig. 2. Schematic presentation of the theoretical energy charging model.

Since the heat capacities of the transparent cover and the air layers are relatively small with respect to the oil and the PCM, and since the time constants for the thermal response of these layers are relatively short with respect to the solar cycle period (Shmidt et al., 1988), only the thermal resistance to heat flow through these layers are taken into account in the ICS-PCM mathematical model. The temperatures of the transparent cover and the air layer are considered to be uniform and time dependent.

Convection heat transfer in the SHTL and the PCM layers is neglected, and transient, one-dimensional heat conduction is assumed. For the PCM layer, it is further assumed that phase transition in the salt hydrate occurs over a range of temperatures. Thus, the PCM layer is divided into three sublayers: a liquid sublayer, a solid sublayer, and the sublayer undergoing phase transition. It is assumed that all the thermophysical properties of the PCM are constant and uniform in each sublayer. However, the specific heat in the phase transition sublayer is an effective thermophysical property including the latent heat effect (Rabin and Korin, 1993).

On the basis of the above-described assumptions, the governing equations in the SHTL and in each of the PCM sublayers are similar and may be presented as:

$$\frac{\partial^2 T_i}{\partial x^2} = \frac{1}{\alpha_i} \frac{\partial T_i}{\partial t} \qquad (1)$$

where i is the layer/sublayer index, which can be: f, ℓ, m or s for the SHTL, liquid PCM, melting PCM, or solid PCM, respectively.

The absorber plate has a relatively low thermal resistance to heat flow (metal) and a very low heat capacity (a thin plate) with respect to the other components. Thus, it is assumed that the absorber plate acts as a time-dependent

plane heat source. Neglecting the thermal mass of the absorber plate, the upper boundary condition for eqn (1) could be obtained from energy balance on the absorption plate, which is given by eqn (2)

$$Ak_f \frac{\partial T_f}{\partial x} + \frac{T_\infty - T_f|_{x=0}}{R_c + R_\infty} + Aaq_r = 0 \qquad (2)$$

where the parameter a is an effective absorption coefficient of the integrated system (measured experimentally), R_∞ is the convective thermal resistance between the surface cover and the environment, which is given by:

$$R_\infty = \frac{1}{h_\infty A} \qquad (3)$$

where h_∞ is the convection heat transfer coefficient (in W m^{-2} K^{-1}) determined from eqn (4), in which U is the wind velocity (in m s^{-1}) (Macadams, 1954):

$$h_\infty = 6.2 + 1.4U. \qquad (4)$$

R_c is the equivalent thermal resistance of both the transparent cover and the stationary air layer between the cover and the absorber plate and is given by:

$$R_c = \frac{b}{k_c A} \qquad (5)$$

where k_c is an effective thermal conductivity coefficient.

The inner boundary conditions at the interfaces between the STHL layer and the PCM sublayers present continuity in temperature and heat fluxes:

$$T_i|_{x=l_i} = T_j|_{x=l_i} \qquad (6)$$

$$-k_i \frac{\partial T_i}{\partial x}\bigg|_{x=l_i} = -k_j \frac{\partial T_j}{\partial x}\bigg|_{x=l_i} \qquad (7)$$

where the index i may represent the layers/sublayers f, ℓ or m, and the index j represents ℓ, m or s, respectively.

The lower boundary condition is presented as a thermal insulation:

$$\frac{\partial T}{\partial x}\bigg|_{x=L} = 0. \qquad (8)$$

The initial temperature distribution is considered to be a function of one dimension and is represented by:

$$T(x, t=0) = g(x) \quad 0 \le x \le L. \qquad (9)$$

The phase change problem defined above using an effective specific heat is based on the

enthalpy approach. Thus, the solution of this problem was performed by a finite difference and enthalpy-based numerical scheme (Rabin and Korin, 1993). This numerical solution was found to be an efficient numerical technique for a mulidimensional problem under various boundary conditions. The proposed solution provides the temperature distribution in the system. However, the locations of the PCM interfaces have to be interpolated from the temperature distribution. Furthermore, it should be noted that there can be one or more interfaces at the initial time.

3. EXPERIMENTAL SETUP

An experimental model of the ICS-PCM system was designed and build for an investigation of the concept and of the mathematical model in the stage of the charging process. The apparatus was designed to simulate a center part of the ICS-PCM prototype, where the heat flow is one-dimensional and where there are no end effects. Thus, the experimental model was designed to have the same height as the prototype system. One-dimensional heat flow in the experimental model was achieved by insulating the model with a thick layer of a material having a very low thermal conductivity coefficient (polyurethane).

A schematic cross-section of the components of the experimental model are shown in Fig. 3. The experimental system consisted of a 10 mm thick Plexiglas container, 0.3×0.3 m in cross-section and 0.131 m in height. The sides of the container were thermally insulated with a 40 mm thick layer of polyurethane. The container was filled with 13.4 kg of a salt hydrate PCM, composed of a eutectic mixture (in wt%) of: 48.0 $CaCl_2$, 4.5 KCl, 0.4 NaCl and 47.1 H_2O, with the addition of 1 wt% $BaCl_2 \cdot 2H_2O$ as a nucleating agent. This PCM has a phase transition temperature interval of 27–29°C, a latent heat of 164.5 kJ/kg, and solid and liquid densities of 1610 and 1490 kg/m^3, respectively (Korin, 1982; Wolf et al., 1984; Korin et al., 1985). Paztherm 22 oil (1460 cm^3), used as the SHTL, was poured onto the PCM in the solid state.

Before each experiment the system was kept in a constant controlled temperature compartment for about three days so that the PCM could solidify completely. Temperatures profiles were measured by copper–constantan thermocouples (type T) mounted on three 3 mm dia Plexiglas bars, each containing five sensors. The container was covered with a metal plate coated with a selective absorber material. A 10 mm thick transparent polycarbonate panel was placed over the cover to provide thermal insulation. The oil that was pushed out of the system during the melting was allowed to flow through 3 mm copper pipes and rubber piping into a 500 ml graduated vessel. By measuring the volume of oil that flowed out of the system the locations of the liquid/solid interfaces were determined, as a function of time, for further validation of the model. A summary of the relevant thermophysical properties of the components of the experimental ICS-PCM system is given in Table 1.

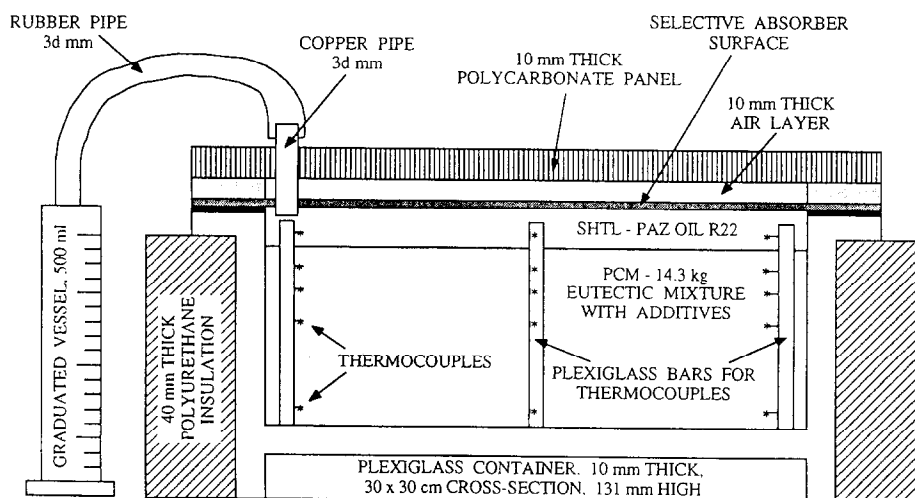Meteorological data (ambient temperature, solar intensity, and wind velocity) were obtained

Fig. 3. Schematic cross-section of the experimental system.

Table 1. Typical thermophysical properties of the materials of the ICS system

Thermal conductivity W m^{-1} K^{-1}	PCM in a liquid phase	0.5†
	PCM in a solid phase	0.6†
	Plexiglas	0.1
	Polyurethane	0.04
	Absorber plate	43
	Air	0.028 (50°C)
	Transparent cover	0.042
	Paztherm 22 (oil)	0.145
Volumetric specific heat MJ m^{-3} K^{-1}	PCM in a liquid phase	4.16†
	PCM in a solid phase	2.88†
	Absorber plate	3.69
	Air	0.0013
	Paztherm 22 (oil)	1.62
Density kg m^{-3}	PCM in a liquid phase	1600†
	PCM in a solid phase	1800†
	Paztherm 22 (oil)	860
Volumetric latent heat MJ m^{-3}	PCM	255†

†Average values of salt hydrates.

from a meteorological station located near the experimental area. The solar energy absorbed by the system was determined by a measurement of the direct and diffuse radiation reflected from the upper surface of the system. Uncertainty of temperature measurements in the experimental apparatus was estimated to be in the range of ±0.5°C.

4. RESULTS AND DISCUSSION

4.1. Experimental validation tests

Several energy charging experiments were conducted in an arid zone area—Beer-Sheva, Israel (31°15′N, 45°34′E, 315 m MSL)—during the wintertime. Results of these experiments were used for validation of the mathematical model as well as for an experimental investigation of the ICS concept.

Typical validation test results of the mathematical model, from one of these experiments conducted on a typical winters day, are given below. Figure 4 presents a comparison of the one-dimensional temperature distribution, as calculated by the numerical solution of the mathematical model, and the measured data. It can be seen that there is a very good agreement between the numerical results and measured data in the PCM sublayers. The numerical solution in the SHTL layer is less accurate, especially in the afternoon, probably due to the fact that the mathematical model neglects heat transfer by convection in this liquid layer. The relatively low accuracy of the numerical solution

in the SHTL has a minor influence on the thermal analysis, since the thermal mass of the SHTL is considerably less than that of the PCM. On the other hand, the high accuracy of the numerical solution in the PCM layer is of major importance, since it helps us in estimating the fraction of the liquid phase in the PCM and thus in estimating the amount of energy stored in the system.

Predicted values for liquid/solid interfaces and the energy stored in the system were in good agreement with experimental data, when considered for engineering design purposes. The results show that on a typical winters day, the salt-hydrate started melting at about 09:30, and the overall daily solar absorption efficiency (defined as the ratio between the total energy absorbed by the PCM and the total daily solar radiation reaching the collector area) was about 70%.

4.2. Parametric studies

The phase transition temperature interval and the thickness of the salt-hydrate PCM layer are important design parameters of the ICS-PCM system. In the determination of the optimal values of these parameters for a specific application both the charging and the discharging processes have to be considered. In the present analysis, the validated theoretical model was used to study the effect of these parameters on the ICS-PCM system during the charging process. In the light of the possible application of night space heating in greenhouses in an arid zone, the study of the phase transition parameter was limited to a range between 15–35°C. The study was performed with a series of PCMs that are based on salt-hydrate mixtures of $CaBr_2 \cdot 6H_2O$ and $CaCl_2 \cdot 6H_2O$. The unique features of these PCMs are: (1) the various mixtures solidify as solid solutions and melt completely over a narrow temperature range of about 2°C to give a homogeneous liquid solution; (2) with suitable nucleating agents the solidification/melting process takes place without going through an incongruent phase transition point, so that the phase change process of these mixtures is totally reversible (Korin, 1982); (3) by selecting a suitable $CaCl_2 \cdot 6H_2O$ to $CaBr_2 \cdot 6H_2O$ weight ratio, it is possible to adjust the transition temperature within a range of 10–34.2°C, while the volumetric heat capacities of the various PCMs remain almost constant. In the theoretical studies presented here we assumed that all phase transitions in the
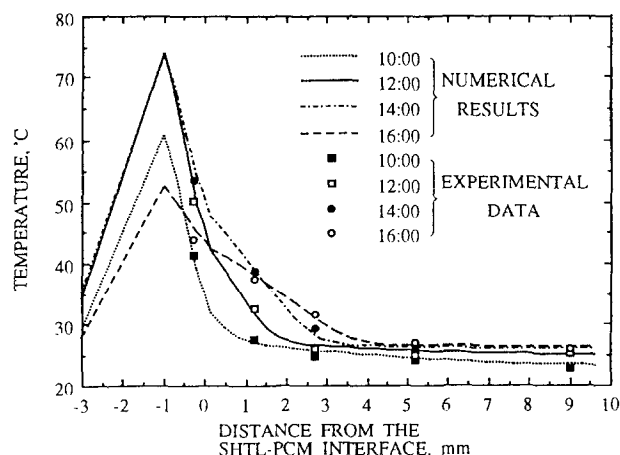
Fig. 4. Comparison between the numerical solution of theoretical model with experimental data, at different times of a typical winter day, Beer-Sheva, Israel.
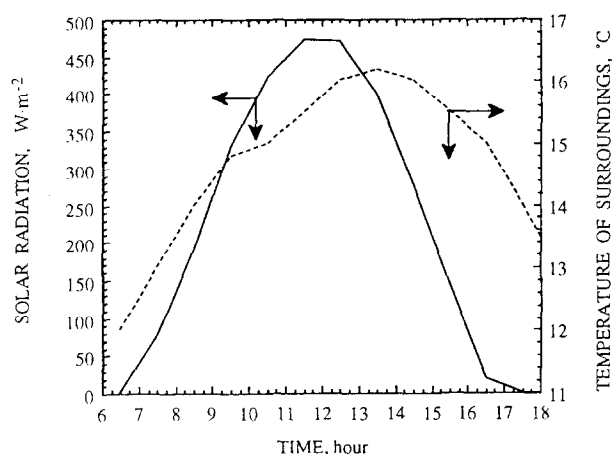

Fig. 5. Meteorological data during the experiment shown in Fig. 4.

PCMs occurred in a $\pm 1°C$ temperature interval around a nominal transition temperature.

All the parametric studies presented here were performed using typical thermophysical properties for salt-hydrates, as presented in Table 1.

Assuming that all the collected daily solar energy is stored as latent heat, the "melted" thickness of the PCM layer could be estimated from the simple equation:

$$l_{pcm} = \frac{\eta \cdot H}{\lambda} \qquad (10)$$

where: l_{pcm} is the thickness of the melted PCM layer, η is the total daily solar collection efficiency, H is the total daily solar radiation and λ is the volumetric latent heat.

The monthly means for the daily total solar radiation in the Beer-Sheva area ranges between $10\ MJ/m^2$ in January and $38\ MJ/m^2$ in June (Kudish and Ianetz, 1992). On the following assumptions: (1) in the period for growing out-of-season winter crops (January–March) the daily total solar radiation might reach a maximum of $25\ MJ/m^2$; (2) all the solar energy collected in the ISC-PCM is stored as latent heat of the PCM; (3) the volumetric latent heat capacity is $255\ MJ/m^3$; and (4) the solar collection efficiency ranges between 65 and 70%, the maximal thickness of that PCM layer that might melt in the winter growing season has to be in the range of 64–69 mm.

As a case study in this analysis we chose to present the results pertaining to the weather conditions of January, which is the coldest month. The thickness of the PCM was chosen to be 67 mm, as this value was found as first estimation for the entire period January to March, for which heating is required in greenhouses. Meteorological parameters were taken from statistical data for January in the Beer-
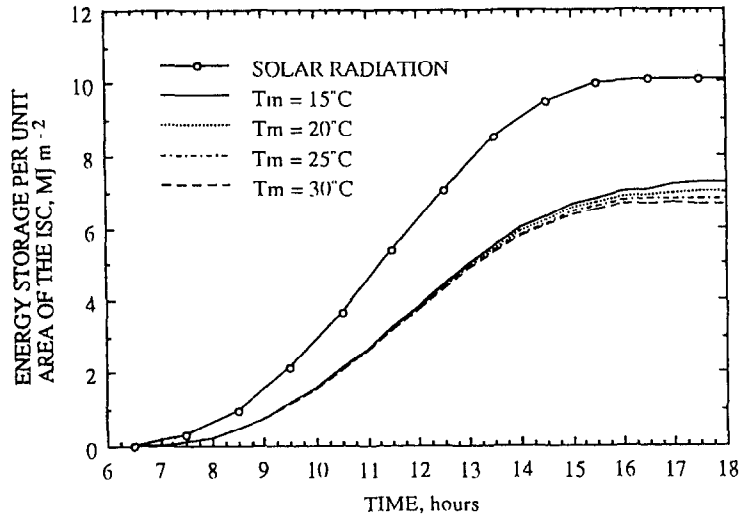
Fig. 6. Thermal energy storage per unit of collector area vs. time of the day for different phase transition temperatures.
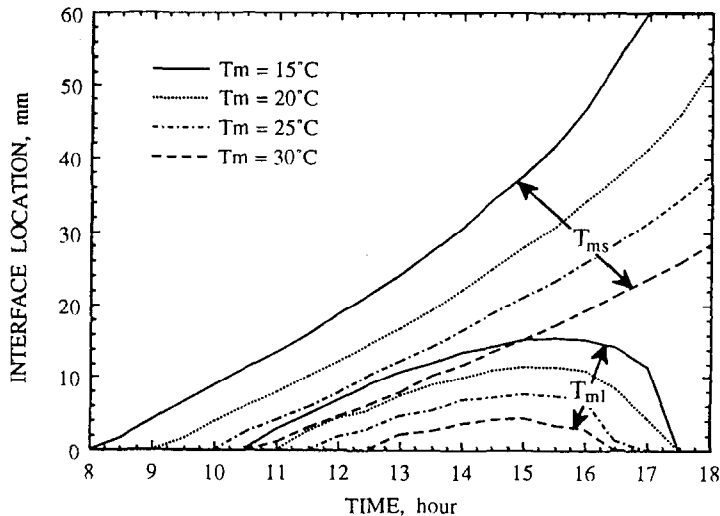

Fig. 7. Location of the interfaces as a function of the time of the day for various phase transition temperatures. T_{ml} and T_{ms} represent the interfaces between the liquid and melting regions and between the melting and solid regions, respectively.

Sheva area, as presented in Fig. 5. The overall absorption coefficient of the absorber metal plate in January was taken as 0.75, which was an average value that was predicted from experimental measurements of the direct and diffuse radiation reflected from the upper surface of the ICS system. The convective heat transfer coefficient to the surroundings was estimated as $15 \text{ W m}^{-2} \text{ K}^{-1}$.

The first parameter to be studied was the nominal melting temperature. As discussed above, the phase transition interfaces of the PCMs were defined by the isotherms $T_m - 1°C$ and $T_m + 1°C$. In terms of the enthalpy

approach, an effective specific heat was assumed to lie between these two isotherms.

The energy stored in the ICS system, as a function of time, and the solar energy transferred to the outer surface of the ICS is shown in Fig. 6. Figure 7 presents the location of the interfaces inside the PCM. From Fig. 6 it can be seen that the melting temperature has only a minor influence on the solar absorption efficiency. For melting temperatures in the range of 15–30°C the solar absorption efficiency is 65–70%. However, from Fig. 7 it can be seen that the melting temperatures have a major influence on the rates of phase change. The
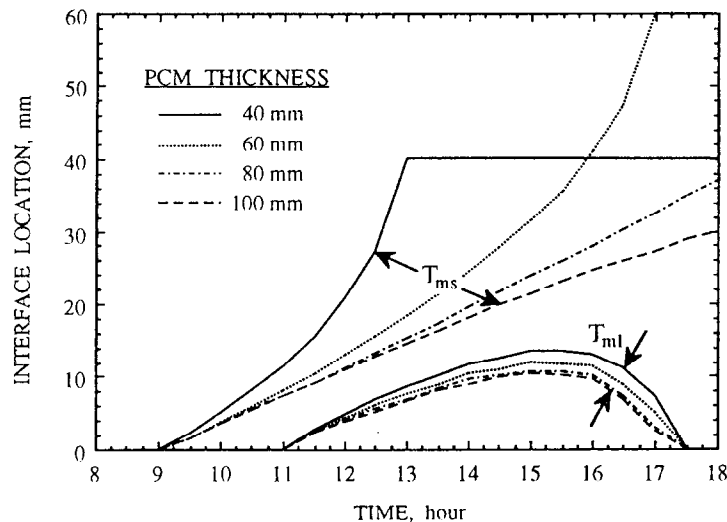
Fig. 8. Location of the interfaces as a function of the time of the day for various thicknesses of the PCM layer. The nominal phase transition temperature is 20°C. T_{ml} and T_{ms} represent the interfaces between the liquid and melting regions and between the melting and solid regions, respectively.

energy charging period may be divided into two stages (Fig. 7) as follows: The first stage can be defined as the period in which the two interfaces propagate in the same direction, towards the bottom of the container. This stage starts later for higher melting temperature materials and ends in the afternoon, approximately at 15:00. The second stage can be defined as the period in which the solar radiation decays and the temperature distribution in the PCM tends to become uniform around its phase transition temperatures. In the second stage the two interfaces propagate in opposite directions. From an examination of the material melting at 15°C, for example, it can be seen from Fig. 7 that by 17:00 the solid front interface reaches the bottom of the container and by 17:30 the liquid front interface returns to the SHTL–PCM interface. Thus, by 17:30 all the PCM is within the phase transition temperature interval. A numerical solution for the same problem with a melting temperature of 35°C is not presented here, since for meteorological conditions of January and a PCM thickness of 67 mm all the energy is stored as sensible heat.

The effect of the thickness of the PCM was studied in the range between 20–100 mm. We chose a nominal melting temperature of 20°C for this parametric study. The locations of the PCM interfaces, as a function of time of the day, for various thicknesses of the PCM are shown in Fig. 8. The maximum propagation distances that the liquid and solid fronts reached during the day for various PCM thicknesses are given in Table 2. The theoretical results showed that for a thickness of 20 mm, the liquid phase front reached the bottom at about 14:30 (Table 2), i.e. all the PCM had completely melted. The maximum propagation of the liquid front increased with decreasing thickness of the PCM layer (Fig. 8 and Table 2). For a thickness range of 30–100 mm this maximum value is reached almost at the same time (15:20) for all cases. With regard to the propagation of the solid phase front, for thicknesses less than 60 mm this front reached to the bottom surface of the PCM layer, while for thicknesses above 70 mm this front did not reach the bottom and the maximum penetration distance decreased with increasing of PCM thickness.

Thus, under the conditions of this study, the

Table 2. Maximal propagation distance of the liquid and solid front interfaces during the day for a nominal melting temperature of 20°C and average meteorological data for January

| PCM layer thickness (mm) | Maximal phase front propagation | | | |
| | Liquid interface | | Solid interface | |
	Distance (mm)	Time of day	Distance (mm)	Time of day
20	20	14:30	20	10:00
30	14.3	15:20	30	11:30
40	13.4	15:20	40	13:00
50	12.5	15:20	50	15:00
60	11.9	15:20	60	17:00
70	11.2	15:20	45.9	18:00
80	10.7	15:20	37.1	18:00
100	10.7	15:20	30.0	18:00

thickness of the PCM layer had a major influence on the location of the propagation distance of the solid interface and a minor influence on the liquid interface. However, it should be noted that both the formation of the interfaces and the disappearance of the liquid phase interfaces took place at the same time for all four cases examined in this study (Fig. 8).

For the particular case study of a nominal transition temperature of 20°C and meteorological data for the coldest month (January), a PCM layer thickness of no more than 30 mm is required to store the daily solar energy.

5. CONCLUSIONS

A new type of ICS system for a low-temperature heat supply has been presented. The ICS system uses a salt-hydrate PCM as a solar energy storage medium. The discharging process is performed by a finned coil heat exchanger located in an organic heat transfer fluid layer (oil) floating above the PCM. The main advantage of this method is that it uses a water/oil heat exchanger in place of an expensive water/salt-hydrate surface heat exchanger. The possible use of this system is limited to special applications, such as space and soil heating of greenhouses located in arid zone areas, during winter.

A simplified theoretical model to study the thermal performance of such a system in the charging process was developed, and an experimental system was set up to validate it. Comparison between mathematical results of the model with experimental data, for the temperature profiles in the salt-hydrate PCM and in the SHTL, and for the location of the solid/liquid interfaces in the PCM as function of time, showed reasonable agreement for engineering design purposes. The comparison also indicated that the model could be improved by taking into consideration the effect of convective heat transfer in the SHTL.

Our experimental study showed that in the winter in Beer-Sheva about two-thirds of the total daily solar energy falling on the collector surface could be collected and stored at 28°C using a PCM based on a eutectic mixture of calcium chloride.

Theoretical study on the effects of the transition phase change temperature (in the range 15–35°C) and the thickness of the PCM layer (in the range 20–100 mm) showed that for the phase transition at 20°C—which is suitable for

heating greenhouses—the PCM thickness for energy collection has to be 30–65 mm. However, the optimal design of this parameter should also take into consideration the discharging process and engineering aspects of the system; this will be undertaken in the future.

NOMENCLATURE

a effective absorption coefficient of the integrated system
A surface area of the collector (m^2)
b transparent cover and air layer thickness (m)
h heat transfer coefficient by convection ($W\,m^{-2}\,K^{-1}$)
H total daily solar radiation (J/m^2)
g initial temperature profile function
k thermal conductivity ($W\,m^{-1}\,K^{-1}$)
l thickness (m)
L the thickness of the solar collector storage system (m)
q heat flux ($W\,m^{-2}$)
R thermal resistance to heat flow ($K\,W^{-1}$)
t time (s)
T temperature (K or °C)
u wind velocity ($m\,s^{-1}$)
x coordinate (m)
α thermal diffusivity ($m^2\,s^{-1}$)
δ interface location (m)
λ volumetric latent heat ($MJ\,m^{-3}$)
η total daily solar collection efficiency

Indexes

c transparent cover and air layer
f stationary heat transfer liquid, SHTL
h convection
i, j layers/sublayer index
ℓ liquid
m melting
r radiation
s solid
∞ surroundings
pcm phase change material

REFERENCES

Bar-Cohen A. Thermal optimization of compact solar water heater. *Solar Energy* **20**, 143–196 (1978).
Barlow D. W. Phase change material heat exchanger. U.S. Pat. 4,219,072 (1980).
Boy E., Boss R. and Lutz M. A collector storage module with integrated phase change material. *Proc. ISES*, Hamburg (1987).
Greene N. D. Energy storage and retrieval as heat. U.S. Pat. 4,109,702 (1978).
Korin E. Investigation of salt-hydrate mixtures for thermal energy storage. Ph.D. thesis, Ben-Gurion Univ., Beer-Sheva, Israel (1982).
Korin E. and Mikic B. Heat transfer improvement in salt hydrate phase change energy storage systems. Report submitted to U.S.–Israel Binational Science Foundation (BSF), Beer-Sheva, Israel. The Institutes for Applied Research, Report no. BGUN-ARI-27-89 (1989).
Korin E. Pasternak D., Rappaport E., Roy A. and Wolf D. A novel passive solar greenhouse based on phase-change materials. *Int. J. Solar Energy* **5**, 201–212 (1987).

Korin E., Rappaport E., Pasternak D., Roy A. and Wolf D. Phase change heat storage building materials. U.S. Pat. 4,498,459 (1985).

Kopel R., Gale J., Zeroni S. and Levi S. A greenhouse with selective radiation filtering under desert conditions. *Proc Int. Symp. Appl. Technol. Greenhouses (91-1STG)*, pp. 63–68, Beijing (1991).

Kudish A. I. and Ianetz A. Analysis of the solar radiation data for Beer-Sheva, Israel, and its environs. *Solar Energy* **48**, 97–106 (1992).

Macadams W. H. *Heat Transmission*, 3rd edn. Mac-Graw–Hill, New York (1954).

MacCracken C. D. PCM bulk storage. *Proc. Int. Conf. Energy Storage*, U.K., pp. 159–164 (1981).

Rabin Y. and Korin E. An efficient numerical solution for the multidimensional solidification (or melting) problem using a microcomputer. *Int. J. Heat Mass Transfer* **36**, 673–683 (1993).

Shmidt C. Goetzberger A. and Shmidt C. Test results and evaluation of integrated collector storage systems with transparent insulation. *Solar Energy* **41**, 487–494 (1988).

Wolf D., Roy A. and Korin E. Heat storage compositions. Isr. Pat. No. 61572 (1984).

Zabeltitz C. V. Greenhouse heating with solar energy. FAO (1987).

Zabeltitz C. V. Passive solar heating of greenhouses with water-filled polyethylene tubes. Greenhouse heating with solar energy. FAO (1989).